

Near-field induction heating of metallic nanoparticles due to infrared magnetic dipole contribution

Pierre-Olivier Chapuis,* Marine Laroche, Sebastian Volz, and Jean-Jacques Greffet

Laboratoire d'Énergétique Moléculaire et Macroscopique, Combustion CNRS UPR 288, Ecole Centrale Paris, Grande Voie des Vignes,
F-92295 Châtenay-Malabry Cedex, France

(Received 12 November 2007; published 6 March 2008)

We revisit the electromagnetic heat transfer between a metallic nanoparticle and a highly conductive metallic semi-infinite substrate, commonly studied using the electric dipole approximation. For infrared and microwave frequencies, we find that the magnetic polarizability of the particle is larger than the electric one. We also find that the local density of states in the near field is dominated by the magnetic contribution. As a consequence, the power absorbed by the particle in the near field is due to dissipation by fluctuating eddy currents. These results show that a number of near-field effects involving metallic particles should be affected by the fluctuating magnetic fields.

DOI: [10.1103/PhysRevB.77.125402](https://doi.org/10.1103/PhysRevB.77.125402)

PACS number(s): 07.79.Fc, 03.50.De, 44.40.+a

I. INTRODUCTION

A lot of attention has recently been devoted to the interaction between nano-objects, such as atoms, nanoparticles or atomic force microscopy tips, and surfaces, which is mediated by fluctuating thermal fields. A great variety of phenomena such as Casimir-Polder forces,^{1–4} friction forces,^{5–9} and near-field heat transfer^{10–26} is governed by the associated stochastic thermal currents. A common assumption is that the electric dipole approximation can be used to model the nano-object.^{18–25} Here, we revisit the heat transfer between a surface and a metallic nanoparticle. We find that the leading mechanism is near-field induction heating due to Joule dissipation of eddy currents in the particle. The large currents are produced by time-dependent infrared magnetic fields that dominate the energy density near a metallic surface. We find a different distance dependence of the flux for noble metals as compared with the case of polar materials. Our work may find applications on local heating for data storage²⁷ and lithography.^{20,28}

All the phenomena previously cited have to be described in the framework of fluctuational electrodynamics introduced by Rytov *et al.*²⁹ It is known that the radiative heat flux between two bodies^{10–19} can be dramatically enhanced when their separation distance becomes smaller than 10 μm . It was found that evanescent waves yield the leading contribution to the heat flux. Experiments have been reported demonstrating these effects.^{30–32} It has also been predicted that this heat transfer could have a very narrow energy spectrum^{16,17,21} due to surface electromagnetic waves. A possible application to design near-field energy converters has been studied.³³

The electric dipole moment of a sphere with radius R and dielectric constant ϵ_r is generally assumed to give the leading contribution^{18–25} because it varies like $(R/\lambda)^3$, whereas the next term in the Mie expansion varies as $(R/\lambda)^5$ (λ is the wavelength in vacuum).³⁴ In this work, we will show that the interaction between the magnetic dipole and the large magnetic fields in the near field may give the dominant contribution to the heat transfer.

In the next section, we compare the absorption cross section of the electric and magnetic dipole moments. The third section is devoted to the analysis of the electric and magnetic

energy densities in the near field of a metal-vacuum interface. The final section analyzes the heat transfer and discusses the physical mechanism.

II. ABSORPTION BY A METALLIC NANOPARTICLE

Let us first compute the power absorbed by a small metallic particle. In what follows, we will use an isotropic, homogeneous, and local form of the complex dielectric constant. To lowest order in R/λ ,³⁴ the particle can be described by its electric dipolar moment \vec{p} . We define a complex polarizability α_E ,

$$\vec{p} = \alpha_E \epsilon_0 \vec{E}, \quad (1)$$

where ϵ_0 is the dielectric vacuum permittivity and \vec{E} is the external electric field. Another contribution is given by the magnetic dipolar moment \vec{m} characterized by its magnetic polarizability α_H ,

$$\vec{m} = \alpha_H \vec{H}, \quad (2)$$

where \vec{H} is the external magnetic field. Higher multipoles can be neglected if $|\epsilon_r| \gg 1$ and $R/\lambda \ll 1$. The contributions of the electric and magnetic dipoles to the power dissipated in the particle at a positive frequency ω are given by^{35,36}

$$P_{abs}^E(\omega) = 2\omega \text{Im}(\alpha_E) \epsilon_0 \frac{\langle |\vec{E}|^2 \rangle}{2}, \quad (3)$$

$$P_{abs}^M(\omega) = 2\omega \text{Im}(\alpha_H) \mu_0 \frac{\langle |\vec{H}|^2 \rangle}{2}, \quad (4)$$

where μ_0 is the magnetic permeability in vacuum. α_E and α_H can be found in Ref. 37,

$$\alpha_E = 4\pi R^3 \frac{\epsilon_r - 1}{\epsilon_r + 2}, \quad (5)$$

$$\alpha_H = \frac{2\pi}{15} R^3 \left(\frac{2\pi R}{\lambda} \right)^2 (\epsilon_r - 1), \quad (6)$$

where ϵ_r is the relative dielectric permittivity.

Here, we do not take into account the diamagnetism of the material. Instead, the magnetic dipole moment is due to eddy currents in the particle. The polarizabilities are calculated assuming that R is much smaller than the skin depth δ . A different form³⁵ can be derived when dealing with particles such that $\delta \ll R \ll \lambda$. In what follows, we should keep in mind that the dipole model is a fair approximation, provided that the distance d between the center of the particle and a surface is much larger than R . Note that we have used for simplicity the extinction cross section of the electric dipole. The exact form of the absorption cross section is discussed in Ref. 38. The difference for a metallic nanoparticle is negligible.

As seen from Eqs. (3) and (4), the absorption is the product of two terms, the imaginary part of the polarizability and the local density of energy. We shall show that for metallic nanoparticles at low frequencies, both terms are larger for the magnetic contribution. Let us first analyze the role of the polarizability. It appears from Eqs. (3)–(6) that for values of the dielectric constant on the order of unity, the electric dipole contribution to losses is much larger than the magnetic one because $R/\lambda \ll 1$. Yet, for values of ϵ_r such that $|\epsilon_r| \gg 1$, as it is the case for metals at low frequencies, the magnetic dipole may provide the leading contribution. The physical reason is that the magnetic fields are continuous at an interface so that they can penetrate in the material. By contrast, the electric field in a spherical particle \vec{E}_{int} is related to the external electric field by $\vec{E}_{int} = [3/(\epsilon_r + 2)]\vec{E}_{ext}$. Surface charges induced at the interface prevent the electric field to penetrate efficiently in the metallic particle. This screening effect takes place on a length scale given by the Thomas-Fermi length. It does not depend on the skin depth.

We consider a nonmagnetic metallic particle characterized by a Drude model $\epsilon_r = 1 - \omega_p^2/(\omega^2 + i\omega\nu)$, where ω_p is the plasma frequency and ν is the damping coefficient. To account for the confinement effects, the bulk dielectric constant ϵ_r (Ref. 39) is corrected by modifying the damping constant $\nu = \nu_0 + A\nu_F/R$, where ν_0 is the bulk damping coefficient, ν_F the Fermi velocity, and A a sample-dependent coefficient. Figure 1 shows $\text{Im}(\alpha_E)$ and $\text{Im}(\alpha_H)$ as a function of circular frequency for two gold spheres with radii $R=5$ nm and $R=10$ nm. It is seen that the electric polarizability is larger than the magnetic polarizability at optical frequencies. As explained before, this is no longer the case at low frequencies (typically smaller than ν), where $\text{Im}(\alpha_H)$ is larger than $\text{Im}(\alpha_E)$.

III. LOCAL DENSITY OF ENERGY NEAR A METALLIC SURFACE

To derive the energy absorbed by a particle in the vicinity of an interface, we need to consider the local densities of energy $\frac{\langle \vec{E} \rangle^2}{2}$ and $\frac{\langle \vec{H} \rangle^2}{2}$. In a vacuum, both contributions are equal. The energy per unit volume $U(z, \omega)$ at a distance z from the interface increases dramatically in the near field due to the presence of evanescent waves, as discussed in Refs. 36 and 40. $U(z, \omega)$ is the product of the local density of states (LDOS) $\rho(z, \omega)$ by the mean energy of a mode $\Theta(\omega, T) = \hbar\omega / [\exp(\hbar\omega/k_B T) - 1]$, where $2\pi\hbar$ is the Planck constant,

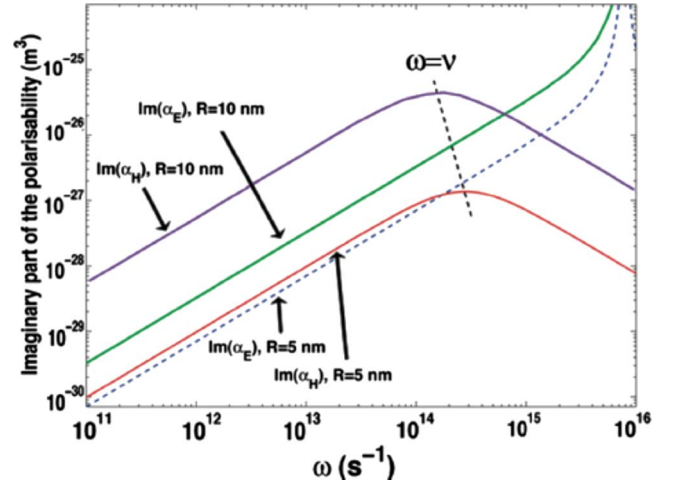


FIG. 1. (Color online) Imaginary parts of the electric and magnetic polarizabilities of a gold sphere ($\omega_p = 1.71 \times 10^{16} \text{ s}^{-1}$, $\nu_0 = 4.05 \times 10^{13} \text{ s}^{-1}$, $\nu_F = 1.2 \times 10^6 \text{ ms}^{-1}$, and $A=1$). For $\omega \ll \nu$, $\text{Im}(\alpha_H) \approx \frac{4\pi R^3 \omega_p^2}{15c^2} \frac{\omega}{\nu}$, and for $\omega \ll \omega_p$, $\text{Im}(\alpha_E) \approx \frac{12\pi R^3 \nu}{\omega_p^2} \omega$.

k_B is the Boltzmann constant, and T is the temperature of the substrate. The final expression for the evanescent part of the LDOS^{36,40} is the sum of the following four contributions:

$$\rho_s^E(z, \omega) = \rho_v \int_{\omega/c}^{+\infty} \frac{dK}{2|\gamma_0|} \frac{cK}{\omega} \text{Im}(r_s) e^{-2\gamma_0'' z}, \quad (7)$$

$$\rho_s^M(z, \omega) = \rho_v \int_{\omega/c}^{+\infty} \frac{dK}{2|\gamma_0|} \frac{cK}{\omega} f(K, \omega) \text{Im}(r_s) e^{-2\gamma_0'' z}, \quad (8)$$

$$\rho_p^E(z, \omega) = \rho_v \int_{\omega/c}^{+\infty} \frac{dK}{2|\gamma_0|} \frac{cK}{\omega} f(K, \omega) \text{Im}(r_p) e^{-2\gamma_0'' z}, \quad (9)$$

$$\rho_p^M(z, \omega) = \rho_v \int_{\omega/c}^{+\infty} \frac{dK}{2|\gamma_0|} \frac{cK}{\omega} \text{Im}(r_p) e^{-2\gamma_0'' z}, \quad (10)$$

where the superscripts E and M denote the electric and magnetic evanescent components, c is the light velocity in vacuum, $\rho_v(\omega) = \omega^2/\pi^2 c^3$ is the vacuum density of states, $f(K, \omega) = 2(\frac{cK}{\omega})^2 - 1$, $r_s = \frac{\gamma_0 - \gamma_1}{\gamma_0 + \gamma_1}$ and $r_p = \frac{\epsilon_{r1}\gamma_0 - \gamma_1}{\epsilon_{r1}\gamma_0 + \gamma_1}$ are the Fresnel TE and TM reflection factors, and the complex number $\gamma_i = \gamma_i' + i\gamma_i''$ is defined as the perpendicular part of the wave vector at a frequency ω : $K^2 + \gamma_i^2 = \epsilon_{ri} \frac{\omega^2}{c^2}$, where $i=0$ in vacuum ($\epsilon_{r0}=1$) and $i=1$ in the metal. We have here neglected non-local effects, but it could be taken into account in the optical reflection coefficients.

In Fig. 2, we plot the LDOS versus the frequency ω for $d=30$ nm. The first conclusion is that the contribution due to the evanescent waves dominates. The second conclusion is that the s -polarized magnetic contribution is dominant for frequencies below $\omega_M = 2.4 \times 10^{14} \text{ s}^{-1}$, which are relevant for heat transfer at 300 K. Indeed, in the expression of the energy density $U(z, \omega)$, $\Theta(\omega, T)$ acts as a temperature-dependent frequency filter. At a given temperature, we define the cutoff frequency ω_M by $\int_0^{\omega_M} \Theta(\omega, T) d\omega / \int_0^{\infty} \Theta(\omega, T) d\omega$

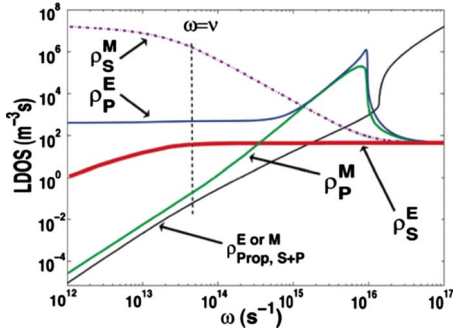


FIG. 2. (Color online) Contributions of the evanescent waves to the local density of states (LDOS) at $d=30$ nm of a gold-vacuum plane interface when using a bulk Drude dielectric constant. The magnetic and electric propagating contributions are also plotted (they are equal).

=99/100. Frequencies much higher than ω_M are not relevant for heat transfer. We note that the p -polarized contribution associated with the surface plasmon polariton dominates at optical frequencies but does not contribute significantly in the infrared.

The dominant contribution of magnetic energy can be understood by considering the analytical expressions of ρ_s^M [Eq. (8)] and ρ_p^E [Eq. (9)]. Both expressions are exactly symmetric, involving the same factor $f(K, \omega)$ and the imaginary part of the reflection factor, respectively, $\text{Im}(r_s)$ and $\text{Im}(r_p)$. The physical origin of the factor $f(K, \omega)$ lies in a fundamental difference of structure between propagating and evanescent waves. It is interesting to see why the magnetic energy dominates the electric energy. Indeed, in a vacuum, the electric and the magnetic energy are equal. This is no longer true for an s -polarized evanescent wave close to an interface.

Let us denote the wave vector as follows:

$$\vec{k}_0 = K\vec{e}_x - \gamma\vec{e}_z, \quad (11)$$

where K and γ are the interface parallel and perpendicular wave vectors and \vec{e}_x and \vec{e}_z are the unit vectors. The Helmholtz equation in a vacuum yields $K^2 + \gamma^2 = \omega^2/c^2$. For an s -polarized field, the electric field is given by

$$\vec{E} = (0, E, 0), \quad (12)$$

and the magnetic field follows from the Maxwell-Faraday equation in vacuum ($\text{curl}\vec{E} = -\frac{\partial}{\partial t}\vec{B}$)

$$\vec{B} = \frac{E}{\omega}(-\gamma, 0, K). \quad (13)$$

It follows that $|\vec{B}|^2 = \vec{B}\vec{B}^* = \frac{|E|^2}{\omega^2}(\gamma^2 + K^2)$. For a propagating wave, this yields the following well-known result:

$$|\vec{B}| = \frac{|\vec{E}|}{c}, \quad (14)$$

whereas for an evanescent wave, γ is purely imaginary so that $|\gamma|^2 = -\gamma^2$. We get

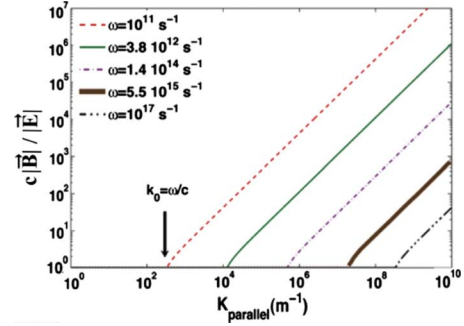


FIG. 3. (Color online) Ratio $\frac{c|\vec{B}|}{|\vec{E}|}$ for s -polarized evanescent waves.

$$\frac{c|\vec{B}|}{|\vec{E}|} = \sqrt{2\frac{K^2}{k_0^2} - 1}. \quad (15)$$

For evanescent waves, $K \gg k_0$, so we find that the magnetic energy stored in an s -polarized evanescent wave is much larger than the electric energy. We have plotted in Fig. 3 the function $\frac{cB}{E} = \sqrt{f(K, \omega)} = \sqrt{\frac{\gamma^2 + K^2}{k_0^2}}$ for different frequencies. It is seen that the density of energy, which is proportional to the density of states, is driven by the magnetic contribution.

Now, a similar reasoning can be done for p -polarized waves. In this case, the inverse ratio $|\vec{E}|/c|\vec{B}|$ is also equal to $\sqrt{f(K, \omega)} = \sqrt{2K/k_0}$, which shows that the electric field dominates in this case. Near field is thus always dominated by an s -polarized evanescent magnetic field and a p -polarized evanescent electric field. The relative weight of both contributions is then given by the values of the imaginary part of the reflection factors. Since $\text{Im}(r_s)$ is larger than $\text{Im}(r_p)$ for a metal at low frequencies, the s -polarized contribution to the LDOS dominates, as seen in Fig. 2. As a consequence, the energy density is dominated by its s -polarized magnetic contribution.

IV. HEAT TRANSFER BETWEEN AN INTERFACE AND A NANOPARTICLE

We now combine the results obtained for the dependence of the polarizabilities and for the energy density to derive the power absorbed by a small particle, as given by Eqs. (3) and (4). Although heat transfer between a small particle and a substrate in the near field has only been calculated using the electric dipolar contribution,^{18–25} the results shown in Fig. 1 (large magnetic dipole moment) and in Fig. 2 (large magnetic density of states) clearly indicate that the magnetic contribution must be taken into account, as suggested in Ref. 32. Figure 4 shows the radiative power

$$P_{rad} = \int_{\omega=0}^{+\infty} [P_{abs}^E(\omega) + P_{abs}^M(\omega)] d\omega \quad (16)$$

dissipated by the substrate in the small particle ($R=5$ nm). The key result observed in Fig. 4 is that the heat transfer is dominated by the s -polarized magnetic contribution. The magnetic contribution can be larger than the electric dipolar

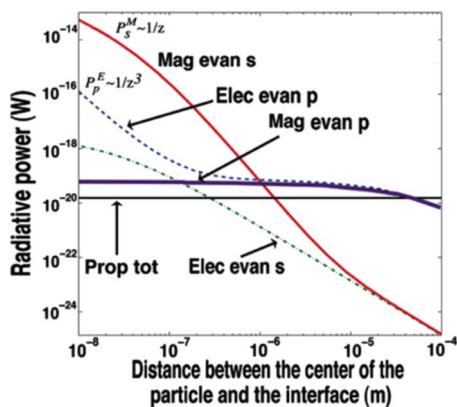


FIG. 4. (Color online) Radiative power dissipated in the gold particle (radius $R=5$ nm) by the semi-infinite planar gold substrate at 300 K, and the asymptotic behaviors.

contribution by 3 orders of magnitude. The reason is that heat is dissipated essentially by eddy currents. An important result is the dependence of the heat flux with distance. The magnetic LDOS varies asymptotically as $1/z$ and the electric LDOS as $1/z^3$.^{36,40} For gold, these behaviors are valid at very small distances (below 20 nm). Hence, there is no simple distance dependence for the absorbed power, as seen in Fig. 4.

The above analysis can be summarized by the following scenario. Random currents flowing parallel to the interface can excite the s -polarized evanescent electromagnetic fields at infrared frequencies. As explained above, the associated magnetic fields take large values in the near field. They are

continuous across a vacuum-metal interface so that they penetrate efficiently in the nanoparticle and can generate large eddy currents. These currents are dissipated through the Joule effect. Thus, thermal heat transfer appears to be due to near-field induction heating. Radiative heat transfer between two parallel metallic surfaces can also be explained with a similar scenario.⁴¹

V. CONCLUSION

In summary, we have shown that the heat transfer between a noble metallic nanoparticle and a noble metallic surface is dominated by the magnetic contribution. Heat is mainly dissipated by fluctuating eddy currents. The widely used electric dipole approximation is valid for dielectrics but breaks down for metals. As a consequence, the $1/z^3$ dependence of the flux between dielectrics is not valid for metals. A number of other effects due to thermal radiation (e.g., forces, friction) between metallic bodies are expected to be driven by their magnetic contribution, even if the media are nonmagnetic. We note that the heat exchanged by two metallic nanoparticles separated by a submicronic distance⁴² should be driven as well by the interaction between their magnetic dipoles.

ACKNOWLEDGMENTS

We thank Karl Joulain and Carsten Henkel for useful discussions. We acknowledge the support of the Agence Nationale de la Recherche under Contract No. ANR06-NANO-062-04.

*olivier.chapuis@centraliens.net

¹H. Failache, S. Saltiel, M. Fichet, D. Bloch, and M. Ducloy, *Phys. Rev. Lett.* **83**, 5467 (1999).
²C. Henkel, K. Joulain, J.-Ph. Mulet, and J.-J. Greffet, *J. Opt. A, Pure Appl. Opt.* **4**, S109 (2002).
³M. Antezza, L. P. Pitaevskii, and S. Stringari, *Phys. Rev. Lett.* **95**, 113202 (2005).
⁴J. M. Obrecht, R. J. Wild, M. Antezza, L. P. Pitaevskii, S. Stringari, and E. A. Cornell, *Phys. Rev. Lett.* **98**, 063201 (2007).
⁵I. Dorofeyev, H. Fuchs, G. Wenning, and B. Gotsmann, *Phys. Rev. Lett.* **83**, 2402 (1999).
⁶J. R. Zurita-Sanchez, J.-J. Greffet, and L. Novotny, *Phys. Rev. A* **69**, 022902 (2004).
⁷A. I. Volokitin and B. N. J. Persson, *Phys. Rev. Lett.* **94**, 086104 (2005).
⁸A. I. Volokitin, B. N. J. Persson, and H. Ueba, *Phys. Rev. B* **73**, 165423 (2006).
⁹G. V. Dedkov and A. A. Khasov, *Europhys. Lett.* **78**, 44005 (2007).
¹⁰E. G. Cravalho, C. L. Tien, and R. P. Caren, *J. Heat Transfer* **89**, 351 (1967).
¹¹D. Polder and M. Van Hove, *Phys. Rev. B* **4**, 3303 (1971).
¹²R. P. Caren, *Int. J. Heat Mass Transfer* **17**, 755765 (1974).
¹³M. L. Levin, V. G. Polvie, and S. M. Rytov, *Sov. Phys. JETP* **6**,

1054 (1980).
¹⁴J. J. Loomis and H. J. Maris, *Phys. Rev. B* **50**, 18517 (1994).
¹⁵A. I. Volokitin and B. N. J. Persson, *Phys. Rev. B* **69**, 045417 (2004).
¹⁶J.-P. Mulet, K. Joulain, R. Carminati, and J.-J. Greffet, *Microscale Thermophys. Eng.* **6**, 209 (2002).
¹⁷C. H. Park, H. A. Haus, and M. S. Weinberg, *J. Phys. D* **35**, 2857 (2002).
¹⁸I. A. Dorofeyev, *J. Phys. D* **31**, 600 (1998).
¹⁹A. I. Volokitin and B. N. J. Persson, *Phys. Rev. B* **63**, 205404 (2001).
²⁰J. B. Pendry, *J. Phys.: Condens. Matter* **11**, 6621 (1999).
²¹J. P. Mulet, K. Joulain, R. Carminati, and J. J. Greffet, *Appl. Phys. Lett.* **78**, 2931 (2001).
²²I. A. Dorofeev, *Tech. Phys. Lett.* **23**, 109 (1997).
²³J. B. Pendry, *J. Mod. Opt.* **45**, 2389 (1998).
²⁴A. I. Volokitin and B. N. J. Persson, *Phys. Rev. B* **65**, 115419 (2002).
²⁵G. V. Dedkov and A. A. Khasov, *Tech. Phys. Lett.* **28**, 50 (2002).
²⁶C. Henkel and M. Wilkens, *Europhys. Lett.* **47**, 414 (1999).
²⁷H. F. Hamann, Y. C. Martin, and H. K. Wickramasinghe, *Appl. Phys. Lett.* **84**, 810 (2004).
²⁸A. Chimmalgi, T.-Y. Choi, C. P. Grigoropoulos, and K. Komvopoulos, *Appl. Phys. Lett.* **82**, 1146 (2003).

- ²⁹S. M. Rytov, Yu. A. Kravtsov, and V. I. Tatarskii, *Principles of Statistical Radiophysics* (Springer, Berlin, 1989), Vol. 3.
- ³⁰C. M. Hargreaves, *Phys. Lett.* **30A**, 491 (1969).
- ³¹W. Müller-Hirsch, A. Kraft, M. T. Hirsch, J. Parisi, and A. Kittel, *J. Vac. Sci. Technol. A* **17**, 1205 (1999).
- ³²A. Kittel, W. Müller-Hirsch, J. Parisi, S. A. Biehs, D. Reddig, and M. Holthaus, *Phys. Rev. Lett.* **95**, 224301 (2005).
- ³³M. Laroche, R. Carminati, and J.-J. Greffet, *J. Appl. Phys.* **100**, 063704 (2006), and references therein.
- ³⁴H. C. Van de Hulst, *Light Scattering by Small Particles* (Dover, New York, 1981).
- ³⁵E. M. Lifshitz, L. D. Landau, and L. P. Pitaevskii, *Electrodynamics of Continuous Media*, 2nd ed. (Butterworth-Heinemann, London, 1984), Chap. 7.
- ³⁶K. Joulain, J. P. Mulet, F. Marquier, R. Carminati, and J. J. Greffet, *Surf. Sci. Rep.* **57**, 59 (2005).
- ³⁷G. W. Mulholland, C. F. Bohren, and K. A. Fuller, *Langmuir* **10**, 2533 (1994).
- ³⁸R. Carminati, J.-J. Greffet, C. Henkel, and J.-M. Vigoureux, *Opt. Commun.* **261**, 368 (2006).
- ³⁹H. Hövel, S. Fritz, A. Hilger, U. Kreibig, and M. Vollmer, *Phys. Rev. B* **48**, 18178 (1993).
- ⁴⁰K. Joulain, R. Carminati, J. P. Mulet, and J. J. Greffet, *Phys. Rev. B* **68**, 245405 (2003).
- ⁴¹P.-O. Chapuis, S. Volz, C. Henkel, K. Joulain and J.-J. Greffet, *Phys. Rev. B* **77**, 035431 (2008).
- ⁴²G. Domingues, S. Volz, K. Joulain, and J.-J. Greffet, *Phys. Rev. Lett.* **94**, 085901 (2005).